11th CONGRESS INTERPRAEVENT 2008

www.interpraevent.at
26-30 May 2008
Dornbirn Vorarlberg Austria

Infrasound Measurements of Mass Movements

A. Kogelnig (1), J. Hübl (1), S.C. Zhang(2), F. Zott (1)

(1) Institute of Mountain Risk Engineering, Department Civil Engineering and Natural Hazards, Universitiy of Natural Resources and Applied Life Sciences, Vienna, Austria
(2) Institute of Mountain Hazards and Environment, Chinese Acadamey of Sciences and Ministery of Water Resources, Chengdu, China

INTERPRAEVENT
International
Research Society

INTRODUCTION

Processes such as avalanches, debris flow, traffic and wind are sources of sub-audible sounds in the low frequency infrasonic spectrum (0-20 Hz). These signals have the ability to propagate kilometers from the source and provide a basis for developing monitoring systems that can operate in locations unaffected by the process activity. However wind creates pressure perturbations that affect infrasonic sensors and introduce noise in acquired data.

Figure 1: The array setup, 8 porous garden hoses encased in a perforated pipe in a star configuration. Top: Summer setup Bottom: Winter setup.

Figure 2: Setup of the infrasound sensors located in a room in the observation station. Left: Gefell Mk 222 Right: Chinese Mk 224.

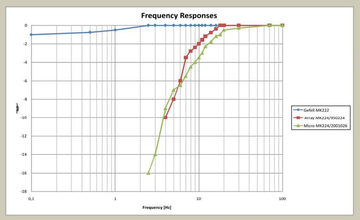

Figure 3: Frequency Responses of the microphones used. The Gefell Mk 222 has the best resolution from 0,1-5 Hz.

AVALANCHES

The results shown in figure 4,5 and 6 have been monitored in March 2007 at the Col du Lautaret (Cemagref Grenoble test side) with the Gefell Mk 222 infrasound sensor and a sampling frequency of 100 Hz. The predominant frequency due to the avalanche, as it appears in Figure 5, is around 4 Hz. Figure 8 shows data of an avalanche triggered at Col du Lautaret in March 2008. To compare and evaluate the signals, they have been recorded simultaneously with two infrasound sensors. One of them was equipped with an array of porous garden hoses as shown in Figure 1; The results (see Figure 7) show clearly that the array could improve the signal to noise ratio; 10 sec after the explosion signals due to the avalanche are visible (see top graph of Figure 7). The picture in the background shows the avalanche of March 2007 (by courtesy of Cemagref Grenoble).

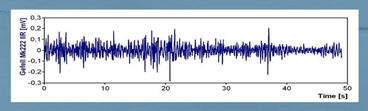

Figure 4: Raw data of the avalanche of March 2007 on Col du Lautaret, France.

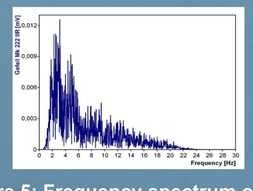

Figure 5: Frequency spectrum of the avalanche of March 2007 on Col du Lautaret , France.

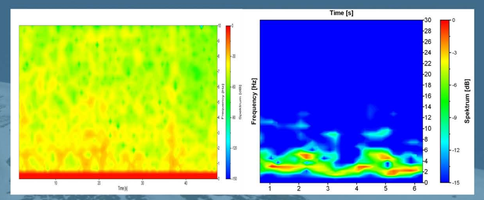

Figure 6: STFT spectrum of unfiltered data (left) and filtered data (right) of March 2007 on Col du Lautaret , France.

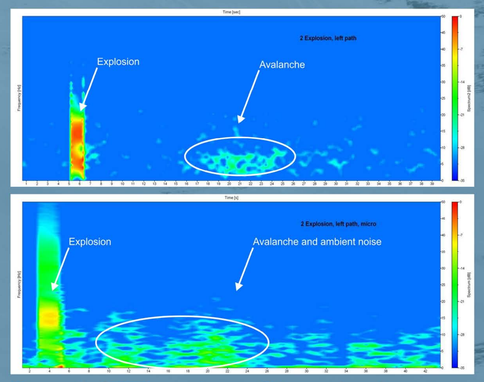

Figure 7: STFT spectrum of the avalanche monitored with array and MK 224/950224 (top), and MK 224/2001026 (bottom); March 2007 on Col du Lautaret , France.

DEBRIS FLOW

The results shown below have been monitored on the 25.07.2007. To compare and evaluate the signals, they have been recorded simultaneously with two infrasound sensors (see Figure 2). On this day, especially in the time between 11.30 am and 1.20 pm, regular debris flow with a density of 2000 kg/m³ was observed. Data were recorded with a sampling frequency of 100 Hz. The predominant frequency, as it appears in Figure 10, is around 10 Hz. There is another peak around 30 Hz, which is not in the infrasonic range. As Figure 9 and 10 illustrate, there are strong correlations throughout the whole analysis between the two different sensors. It is also possible to detect single surges passing the sensor (see Figure 13). Therefore infrasound can be used to detect and record debris flow for warning and research purposes. But also other artificial processes produce infrasonic signals; Thus it is needed to distinguish them from debris flow before.

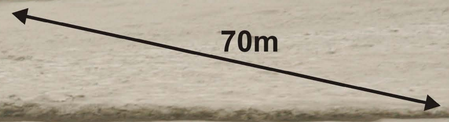

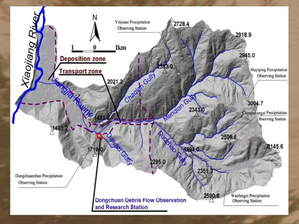

Figure 8: Catchment of the Jiangjia Ravine.

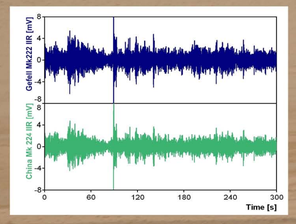

Figure 9: Raw data of Gefell Mk 222 (top) and China Mk 224 (bottom).

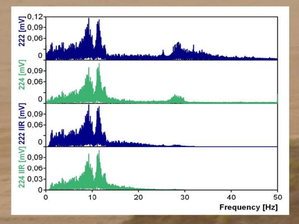

Figure 10: Frequency spectrum of the unfiltered data (top) and filtered signal (bottom).

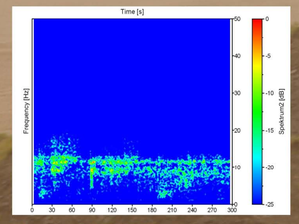

Figure 11: STFT spectrum of filtered data recorded by Mk 222.

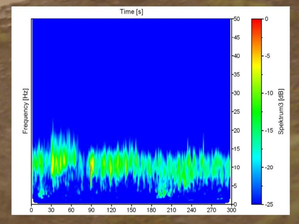

Figure 12: Wavelet spectrum of filtered data recorded by Mk 222.

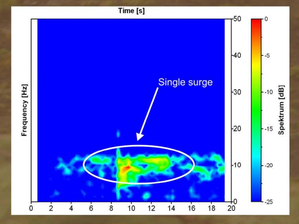

Figure 13: FFT spectrum of filtered data of a single surge recorded by Mk 222.